Draft version October 27, 2016
Preprint typeset using LaTeX style emulateapj v. 5/2/11

arXiv:1610.08055v1 [astro-ph.HE] 25 Oct 2016

THE HIGHEST-ENERGY COSMIC RAYS CANNOT BE DOMINANTLY PROTONS FROM STEADY SOURCES

Ke Fang
Department of Astronomy, University of Maryland, College Park, MD, 20742-2421, USA and
Joint Space-Science Institute, College Park, MD, 20742-2421

Kumiko Kotera
Sorbonne Universités, UPMC Univ. Paris 6 et CNRS, UMR 7095,
Institut d'Astrophysique de Paris, 98 bis bd Arago, 75014 Paris, France and
Laboratoire AIM-Paris-Saclay, CEA/DSM/IRFU, CNRS, Universite Paris Diderot, F-91191 Gif-sur-Yvette, France
Draft version October 27, 2016

ABSTRACT

The bulk of observed ultrahigh energy cosmic rays could be light or heavier elements, and originate from an either steady or transient population of sources. This leaves us with four general categories of sources. Energetic requirements set a lower limit on single source luminosities, while the distribution of particle arrival directions in the sky sets a lower limit on the source number density. The latter constraint depends on the angular smearing in the skymap due to the magnetic deflections of the charged particles during their propagation from the source to the Earth. We contrast these limits with the luminosity functions from surveys of existing luminous steady objects in the nearby universe, and strongly constrain one of the four categories of source models, namely, steady proton sources. The possibility that cosmic rays with energy $> 8 \times 10^{19}$ eV are dominantly pure protons coming from steady sources is excluded at 95% confidence level, under the safe assumption that protons experience less than 30° magnetic deflection on flight.

1. INTRODUCTION

The mystery of the origin of ultrahigh-energy cosmic rays (UHECR) remains unsolved (Kotera & Olinto 2011). Observationally, one major obstacle stems from the lack of convergence on the measured chemical composition at the highest energies. The two leading UHECR observatories report puzzling results: while the Pierre Auger Observatory in the southern hemisphere finds medium to heavy composition above 50 EeV (1 EeV = 10^{18} eV) (Aab 2015), the Telescope Array in the northern hemisphere reports that the composition of particles above EeV is consistent with pure proton (Fukushima 2015).

From a theoretical point of view, many promising UHECR candidate sources have been proposed in the literature. The extreme energy of UHECRs sets a lower limit on the bolometric luminosity of their accelerators (Waxman 1995). But none of the objects passing that cut has been tested conclusively yet – positively or negatively. Based on their decay timescale, they can be grouped into two categories: steady and transient sources. A source can be categorized as steady if its emission timescale is longer than the spread in the arrival time of their UHECRs (Waxman & Loeb 2009; Takami & Murase 2012). In this case, the arrival directions of UHECRs can directly trace and constrain the sky distribution of their sources, in conjunction with other neutral messengers like photons, neutrinos and gravitational waves. Such a spread is caused by magnetic deflections of charged cosmic rays in Galactic and intergalactic media, which can be quantified as $\delta t \approx 10^5 \, (l/100\,\mathrm{Mpc}) \, (\alpha/2^\circ)^2$ yrs (Kotera & Lemoine 2008), for a propagation distance l and a total deflection angle α. We note that the definition of steadiness is relative and dependent on l and α. For protons, α is typically a few degrees (as will be discussed at the end of Section 2). Thus δt ranges from a few tens of years for a Galactic or local source, to $\gtrsim 10^4$ years for a source at the GZK horizon (Greisen 1966; Zatsepin & Kuzmin 1966, also see Section 2). Examples of potential steady sources include radio-loud active galactic nuclei (AGN), quasar remnants, and cluster accretion shocks. Examples of transient candidates include gamma-ray bursts, fast-rotating neutron stars, and giant AGN flares (see Kotera & Olinto 2011 and references therein).

The sources of UHECRs can thus be grouped into four major categories: steady proton, steady heavy nuclei, transient proton and transient heavy nuclei sources. This letter examines whether the measured highest-energy cosmic rays could be protons from steady sources, by comparing the luminosity functions from surveys of luminous steady objects in the nearby universe with the required levels of number density and luminosity of UHE proton sources. We exclude at 95% confidence level (C. L.) the possibility that the observed highest-energy events could be dominated by pure protons from steady sources, under robust assumptions on the magnetic deflections experienced by particles during their propagation. The remaining choices for sources of UHECRs are thus either steady accelerators of heavy elements or transients.

2. LUMINOSITY AND NUMBER DENSITY CONSTRAINTS

Above 60 EeV, observable sources must lie within the so-called GZK horizon, due to energy losses via interactions between extragalactic cosmic rays and the cosmic background radiation (Greisen 1966; Zatsepin & Kuzmin 1966). The horizon is of order $100 - 200\,\mathrm{Mpc}$ at 60

EeV, implying that particles at the highest energies are produced in an anisotropic Universe. However, the arrival directions of observed UHECRs do not display any significant clustering other than in the Telescope Array hotspot region (Abbasi et al. 2014) and the Centaurus A region (Abreu et al. 2010). The lack of strong anisotropy sets lower bounds on the number density of sources, depending on the assumed magnetic deflection of particles (Abreu et al. 2013).

Using the level of clustering in the sky of selected events with energy thresholds of 60, 70, and 80 EeV, the Auger Collaboration derived lower bounds on the source number density of $n_s \sim (0.06-5)\times10^{-4}\,\mathrm{Mpc}^{-3}$ at 95% C. L., if sources are uniformly distributed and equally luminous (Abreu et al. 2013). Similar 95% C. L. bounds of $\sim (0.2-7)\times10^{-4}\,\mathrm{Mpc}^{-3}$ were derived for sources following local matter distribution. These bounds are subject to a factor of 3 uncertainty due to systematic errors on the cosmic-ray energy calibration. The ranges quoted for the bounds correspond to different assumed magnetic deflections. The most (least) stringent bound was obtained for the angular scale $\alpha = 3^\circ$ ($\alpha = 30^\circ$).

The lower bounds on the magnetic luminosity of an UHECR source haven been studied in e.g., Waxman (1995); Lemoine & Waxman (2009). The magnetic power contained in the magnetized plasma of an astrophysical source can be written as $L_B = \beta c\, u_B\, 4\pi\, R_{\rm acc}^2$, where βc is the speed of the magnetic flow, $u_B = B^2/4\pi$ is the magnetic energy density, and $R_{\rm acc}$ is the size of the acceleration region. The potential drop generated by the moving plasma is given by $V = \beta B R_{\rm acc}/\Gamma$, where $\Gamma = \left(1-\beta^2\right)^{-1/2}$ is the Lorentz factor of the relativistic flow, and $R_{\rm acc}/\Gamma$ is the effective size of the acceleration region, considering that the available time in the comoving frame is shortened by Γ. A charged particle passes the acceleration region would gain energy $E_{\rm CR} \le Ze\beta B R_{\rm acc}/\Gamma$. This sets a general lower bound to the magnetic luminosity

$$L_B \ge \frac{\Gamma^2 c}{\beta}\left(\frac{E}{Ze}\right)^2 > 2\times10^{45}\left(\frac{E}{Z\,80\,\mathrm{EeV}}\right)^2 \mathrm{erg/s}\ . \quad (1)$$

Note that equation (1) is a universal argument regardless of the acceleration mechanism or geometry of the acceleration region (Lemoine & Waxman 2009). The term Γ^2/β is larger than unity for a non-relativistic or sub-relativistic source, and is comparable to the beaming factor $\sim\Gamma^{-2}$ in case of a relativistic outflow, hence the second inequality. The equipartition hypothesis suggests an equality of the energies in relativistic particles and magnetic field (Longair 2011). For most astrophysical objects, especially those not dominated by non-thermal emissions, L_B is not expected to exceed the bolometric luminosity, $L_{\rm bol}$. This can be violated if the source is dominantly powered by Poynting flux, and the majority of the magnetic energy is not dissipated into radiation.

In light of these requirements, we perform a census of the luminosity functions (LF) of known bright sources in relevant wavebands and report them in Figure 1. For a conservative comparison and to take into account the uncertainty arising from the conversion of the luminosity in observed bands to L_B for some sources, we consider a cumulative luminosity function. In the plot, the reported luminosities are assumed to be representative of the magnetic luminosity, under the equipartition hypothesis. The issues related to such an assumption, and to the luminosity conversions are discussed below.

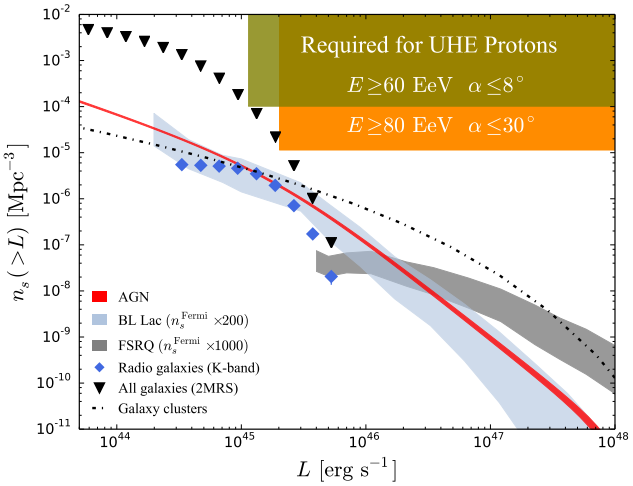

FIG. 1.— Source number density and luminosity required by UHECR observations, assuming that cosmic rays are protons from steady sources (shaded in orange and green boxes), compared to the cumulative luminosity functions of bright galaxies in the nearby universe (black triangle markers) (van Velzen et al. 2012; Rouillé d'Orfeuil et al. 2014), AGN from X-ray surveys (red band) (Ueda et al. 2014), radio galaxies (blue diamond makers) (van Velzen et al. 2012), BL Lac objects (light blue shaded band) (Ajello et al. 2014) and flat spectrum radio quasars (grey shaded band) (Ajello et al. 2012) observed by the Fermi Telescope (Ackermann et al. 2011), and galaxy clusters (dash-dotted black line). The reported luminosities are assumed to be representative of the magnetic luminosity (see text for discussion). The lower bound on the source number density at 95% C. L. is obtained assuming a deflection angle of UHECRs $\alpha \le 8^\circ$ (green), and $\le 30^\circ$ (orange). The lower limit on the source luminosity corresponds to the magnetic luminosity of a source that can accelerate particles to ≥ 60 (green) and ≥ 80 (orange) EeV (Eq. 1).

3. COMPARISON WITH LUMINOSITY FUNCTIONS FROM SURVEYS

The 2MASS Redshift Survey (2MRS) (Huchra et al. 2012) maps the all-sky three-dimensional distribution of galaxies in the nearby universe in the near infrared band. It is the best survey that describes the matter distribution in the nearby universe, and it provides a general measurement of the distribution of bright sources regardless of specific source types. The K-band all-galaxy LF (van Velzen et al. 2012; Rouillé d'Orfeuil et al. 2014) derived from the catalog is indicated as black triangle markers in Figure 1 (using a cosmological constant $h = 0.678$ (Planck Collaboration et al. 2015)).

A complete X-ray LF of AGN was provided by Ueda et al. (2014), utilizing combined samples from surveys performed with Swift/BAT, MAXI, ASCA, XMM-Newton, Chandra and ROSAT. The bolometric luminosity of AGNs can be derived from the X-ray luminosity by a luminosity-dependent bolometric correction (Hopkins et al. 2007). The bolometric LF for AGNs in the local universe is shown as a red band in Fig 1, taking $\Omega_m = 0.308$ (Planck Collaboration et al. 2015) and assuming a flat Universe. An alternative bolometric correction obtained from simultaneous optical-to-X-ray spectral energy distributions of hard X-ray-selected local

AGNs (Vasudevan et al. 2009) leads to a similar LF.

Among the galaxy population, radio-loud active galaxies have been suggested to satisfy necessary preconditions to accelerate and confine UHECRs (e.g. Hillas 1984). An all-sky catalog of extragalactic radio sources of the local universe is provided by van Velzen et al. (2012). The catalog was obtained by matching radio-emitting galaxies from existing radio catalogs, including surveys from NVSS (Condon et al. 1998) at 1.4 GHz and SUMSS (Bock et al. 1999; Mauch et al. 2003) at 843 MHz, with galaxies from the 2MRS (Huchra et al. 2012). The K-band LF for powerful radio galaxies in this catalog ($L > 10^{24}\,\mathrm{W\,Hz^{-1}}$) is shown by blue diamond markers in Figure 1. Radio galaxies constitute about 20% of the total galaxy population above $\sim 10^{45}\,\mathrm{erg\,s^{-1}}$ (van Velzen et al. 2012). We caution that the relationship between the electromagnetic energy of radio-galaxies and radio/near infrared observations is unknown. Allowing for modeling uncertainties, the LF could be significantly shifted horizontally. Although the standard scenarios favor $L_B < L_{\rm bol}$ (e.g., Merloni & Heinz 2007), Poynting-flux dominated models also exist (e.g., Nakamura et al. 2008). An order of magnitude shift with $L_B \sim 10\,L_{\rm bol}$ would however not change our conclusions.

Blazars represent an extreme subclass of the radio-loud AGN, with a relativistic jet pointing along the line of sight of the Earth. Due to their extremely powerful jets, the γ-ray luminosity of blazars could be comparable or even higher than the total luminosity in other bands (Sambruna et al. 1996). The Fermi Telescope has provided the largest sample of blazars to date in γ-rays (Ackermann et al. 2011). LFs of flat spectrum radio quasars (FSRQs) and BL Lacertae (BL Lac) objects have been derived using the γ-ray-selected blazars (Ajello et al. 2012; Ajello et al. 2014). Due to relativistic beaming, only a small fraction of these objects can be observed from the Earth. FSRQs are most seen within 5° of the jet axis with a peak at 2°, while BL Lac objects are most seen within 10° of the jet axis with a peak around 5° (Ajello et al. 2012; Ajello et al. 2014). Assuming a random distribution for the angle between a jet axis and the line of sight ($P(\theta) = \sin(\theta)$ with θ being the viewing angle), the observed FSRQ and BL Lac samples represent $\sim 0.1\%$ (Ajello et al. 2012) and $\sim 0.5\%$ of the parent population. As opposed to photons, UHECRs from an off-aligned AGN could still be deflected in the magnetic field later during their propagation and be reorientated into the direction of the Earth. Therefore a fraction of the off-aligned AGNs could also contribute to UHECRs, depending on the level of deflection. In Figure 1 we take the Fermi LFs of FSRQ and BL Lac objects de-evolved at redshift 0 and multiple their number density by 1000 and 200 respectively to estimate the LF of the entire blazar population. Note that due to the large uncertainties in the LFs from Ajello et al. (2012) and Ajello et al. (2014) we choose to show $n(L)$ instead of $n(>L)$ in Figure 1. The difference is however negligible. The amplified γ-ray LF is consistent with the LF of radio galaxies, and comparable to the bolometric LF of the entire AGN population within uncertainties, implying a common population, as suggested by the unification scenario (Urry & Padovani 1995). Because UHE protons are not expected to deflect completely isotropically and only a fraction of the Fermi blazars are possibly hosting hadronic processes, the amplified LF represents an upper limit to what can be reached by the sources of UHECRs. It is again unclear whether blazar outflows are dominated by kinetic or Poynting-flux power, and whether the magnetic luminosity exceeds the bolometric (see Celotti & Ghisellini 2008 and refs. therein), but our results remain valid within an order of magnitude shift of the LF.

Another type of steady candidate is galaxy clusters (Hillas 1984). The upper limit on the energy of the turbulent magnetic field is determined by the rate of accretion of matter onto the cluster. The total accretion energy reads $L_{\rm acc} = f_b\,GM\dot{M}/r_{\rm vir}$ (Murase et al. 2008; Fang & Olinto 2016), where $f_b = 0.13\,(M/10^{14}M_\odot)^{0.16}$ is the average baryon fraction of galaxy clusters (Gonzalez et al. 2013), and $r_{\rm vir}$ is the virial radius of the cluster. The mass accretion rate is confined by observations as $\langle\dot{M}\rangle(z=0) = 42\,(M/10^{12}\,M_\odot)^{1.13}\,\mathrm{M_\odot\,yr^{-1}}$ (McBride et al. 2009). The corresponding number density is obtained by integrating the cluster halo mass function (Sheth & Tormen 1999) at redshift 0.

In Figure 1 we contrast the above LFs with the region where sources must belong in order to produce the highest-energy cosmic ray protons. The orange box, corresponding to steady proton sources above 80 EeV, comes directly from the least stringent bound of Abreu et al. (2013) (for deflection angles of 30°) and is disjoint from all the observed LFs. The green box in Figure 1 corresponds to sources of particles with energy above 60 EeV, that experience magnetic deflections of $\alpha \leq 8^\circ$. Its lower limit on n_s was chosen by scanning over the range of deflection angles explored by Abreu et al. (2013) and selecting the lowest density allowed at 95% C.L. that does not overlap with the 2MRS luminosity function. Note that, as we discuss below, larger deflection angles would lead to an overlap of the allowed region with a 2MRS population of galaxies that are not expected to be sources of UHECRs. Deflections of $\alpha \leq 22^\circ$ would be allowed if matching the lower limit to the AGN LF.

The level of UHECR deflection depends mainly on the strength and configuration of the extragalactic magnetic fields, which are highly uncertain. The observational bounds that have been placed on the global field strength B and coherence length λ cover a wide range: $B\lambda^{1/2} \in [10^{-19} - 10^{-8}]\,\mathrm{G\,Mpc^{1/2}}$ (Ryu et al. 1998). Heavy numerical simulations of the cosmic magnetic fields and of particle propagation lead to discrepant results (e.g., Das et al. 2008), and often fail at modeling adequately the diffusion of particles due to computational limitations. Semi-analytical models can be used however to infer that a standard set of Galactic and extragalactic magnetic fields should lead to proton deflections of order a few degrees above GZK energies (Waxman & Miralda-Escudé 1996; Kotera & Lemoine 2008).

Quantitatively, the deflection that particles of energy E and charge Z experience due to a homogeneous intergalactic magnetic field with strength B and coherence length λ over a distance d reads $\alpha \sim 6.3^\circ\,Z(E/60\,\mathrm{EeV})^{-1}(d/100\,\mathrm{Mpc})^{1/2}(\lambda/\mathrm{Mpc})^{1/2}(B/\mathrm{nG})$ (Waxman & Miralda-Escudé 1996). If magnetic inhomogeneities are taken into account for a more realistic modeling, the deflection can be expressed as (Kotera &

Lemoine 2008):

$$\alpha \sim 2^\circ\, Z \left(\frac{E}{60\,\mathrm{EeV}}\right)^{-1} \left(\frac{\tau}{3}\right)^{1/2} \left(\frac{r_\mathrm{i}}{2\,\mathrm{Mpc}}\right)^{1/2} \times \left(\frac{B_\mathrm{i}}{10\,\mathrm{nG}}\right) \left(\frac{\lambda_\mathrm{i}}{0.1\,\mathrm{Mpc}}\right)^{1/2}, \quad (2)$$

where magnetized regions (such as filaments, radio ghosts, clusters of galaxies), are characterized by their typical size r_i, magnetic field coherence length λ_i and strength B_i. Trans-GZK particles propagating in the intergalactic medium typically encounter a number $\tau \sim 3$ of such regions (Kotera & Lemoine 2008). The propagation in the Galactic magnetic field results in an additional deflection of α_Gal, the quadratic sum of the turbulent (α_turb) and regular (α_reg) components. Numerically, $\alpha_\mathrm{turb} \sim 0.5^\circ\, Z(E/60\,\mathrm{EeV})^{-1}(H_\mathrm{Gal}/2\,\mathrm{kpc})^{1/2}(\lambda_\mathrm{Gal}/50\,\mathrm{pc})^{1/2} \times (B_\mathrm{Gal,turb}/3\,\mu\mathrm{G})$, where B_Gal, $\lambda_\mathrm{Gal,turb}$ and H_Gal are the magnitude, coherence length, and height of the turbulent component of the Galactic magnetic field, and $\alpha_\mathrm{reg} \sim 3.5^\circ\, Z(E/60\,\mathrm{EeV})^{-1}(L_\mathrm{Gal}/2\,\mathrm{kpc})(B_\mathrm{Gal,reg}/2\,\mu\mathrm{G})$, for a field coherent over lengthscale L_Gal and of strength $B_\mathrm{Gal,reg}$ (Kachelrieß et al. 2007). The above values for the Galactic field are only indicative, and larger deflections up to $\sim 10^\circ$ could be obtained for other configurations of the magnetic field within the observationally constrained range (Haverkorn 2015). Overall deflections of $\leq 8^\circ$ for protons, as quoted above, can thus be viewed as highly reasonable, and $\leq 30^\circ$ is extremely robust.

4. CONCLUSION AND DISCUSSION

The requirements for the production of cosmic ray protons at the highest energies in terms of source luminosity and number density are tight enough to exclude steady candidate sources. Because the observational constraints on the source number density depend on the particle deflection angles, this exclusion relies on the comfortable assumption that protons are deflected of $\leq 30^\circ$ above 80 EeV. Our 95% C. L. on the exclusion directly results from the allowed n_s region (for a given deflection angle) quoted by Abreu et al. (2013). We stress that because our exclusion statements are directly related to the deflection angle, they are not subject to the large uncertainties and subtle details of magnetic field measurements. The luminosity limit is a theoretical pre-requisite and does not have a C. L. attached.

The K-band LF from the 2MRS survey was used as an estimation to the bolometric LF of normal galaxies. If L_bol were significantly higher than $L_\mathrm{K-band}$ (which is possible for some subset of the galaxy population, especially those with strong star formation activities), our conclusion would still be valid with reasonably smaller deflection angles. Notice that the population of sources dominating a K-band survey sample above $L \sim 10^{45}$ erg/s are known to be mostly passively-evolving, early-type galaxies, located at the center of galaxy clusters (e.g., Bonne et al. 2015). In spite of their energy budget, their quiescence and the absence of associated high-energy emission makes them very difficult to reconcile with the production of UHECRs.

The exclusion of steady proton sources could appear even stronger if the boxes were compared to the LFs of radio galaxies and blazars, from which high-energy emission has been detected, and the constraints on the deflection angles would be much relaxed. We recall that the bounds on the source number density reported in Figure 1 are the conservative values quoted by Abreu et al. (2013) for an uniform source distribution. The constraints on n_s would be $\sim 3-10$ times better if considering the inhomogeneous distribution of the local structures. This effect is however absorbed by the uncertainties due to the energy calibration of the observed cosmic rays, that leads to uncertainties of the same order (Abreu et al. 2013). The major unknown remains however the relationship between the bolometric and the magnetic luminosities of the source. If the latter dominates significantly (and if this property is shared by a large fraction of sources within a given population), the LFs would have to be shifted to the right for an accurate comparison with the proton steady source box.

Our conclusions concern the dominant sources of UHECRs and does not exclude the existence of a steady source contributing to the observed spectrum at a minor rate, that would not affect the anisotropy analysis of Abreu et al. (2013).

If one alleviates the primary proton assumption, lower luminosity sources would pass the cut (Eq. 1), enlarging the allowed parameter space to the left in Fig. 1. As for the source number density, Abreu et al. (2013) comments that, although their analysis was performed using protons, the propagation of iron nuclei leads to similar results (for given deflection angles) because the energy loss rates due to photo-disintegration of iron nuclei on cosmic backgrounds are comparable to those of protons. The deflections being stronger for iron than for protons, one expects steady sources of heavy nuclei primaries to be comfortably allowed as UHECR producers.

Due to severe energy losses via photo-hadronic interactions with the cosmic photons, above ~ 60 EeV, only protons and iron-like heavy elements can survive propagation over distances larger than ~ 50 Mpc (see, e.g., Fig. 3 of Kotera & Olinto 2011). Intermediate mass primary nuclei can reach the Earth only if produced very nearby (for carbon-nitrogen-oxygen nuclei, 90% should come from distances ≤ 40 Mpc, and 50% from ≤ 20 Mpc. For helium nuclei, almost 100% should come from ≤ 12 Mpc). Considering that the mass distribution is highly structured in the very nearby universe, tighter bounds on the source number density are expected for intermediate nuclei, leading to a similar exclusion in spite of the relaxed luminosity bound.

Hence, the highest-energy cosmic rays are either iron-like heavy nuclei produced in steady sources, or generated in transient sources.

It is currently difficult to discriminate between the remaining three scenarios. Anisotropy studies with increased statistics from next-generation UHECR observatories should be able to constrain steady source populations, even for heavy nuclei composition (Rouillé d'Orfeuil et al. 2014; Oikonomou et al. 2015). Anisotropy signatures expected from transient source scenarios are less straightforward to interpret than for steady candidates due to the time delay caused by magnetic deflections. Many studies can be found on the subject (Murase & Takami 2009; Kalli et al. 2011) but

the ultimate probe of transient candidates will likely be a multi-messenger transient signal.

Acknowledgements. We thank Kohta Murase, Aurélien Benoit-Lévy, Stéphane Charlot, Guilhem Lavaux, Cole Miller, Richard Mushotzky, Paolo Privitera, and Joe Silk for helpful comments. K.F. acknowledges the support of a Joint Space-Science Institute prize postdoctoral fellowship. K.K. acknowledges support from the PER-SU fellowship at Sorbonne Universités and from the Labex ILP (reference ANR-10-LABX-63, ANR-11-IDEX-0004-02). K.K. thanks the KICP and the University of Chicago for its kind support and hospitality.

REFERENCES

Aab, et al, The Pierre Auger Observatory: Contributions to the 34th International Cosmic Ray Conference (ICRC 2015)
Abbasi, R. U., et al. 2014, Astrophys. J., 790, L21
Abreu, P., Aglietta, M., Ahn, E., Allard, D., Allekotte, I., et al. 2010, Astroparticle Physics, 34, 314
Abreu, P., et al. 2013, JCAP, 1305, 009
Ackermann, M., Ajello, M., Allafort, A., et al. 2011, ApJ, 743, 171
Ajello, M., Shaw, M. S., Romani, R. W., Dermer, C. D., Costamante, L., King, O. G., Max-Moerbeck, W., Readhead, A., Reimer, A., Richards, J. L., & Stevenson, M. 2012, ApJ, 751, 108
Ajello, M., et al. 2014, Astrophys. J., 780, 73
Bock, D. C.-J., Large, M. I., & Sadler, E. M. 1999, The Astronomical Journal, 117, 1578
Bonne, N. J., Brown, M. J. I., Jones, H., & Pimbblet, K. A. 2015, ApJ, 799, 160
Celotti, A., & Ghisellini, G. 2008, MNRAS, 385, 283
Condon, J. J., Cotton, W. D., Greisen, E. W., Yin, Q. F., Perley, R. A., Taylor, G. B., & Broderick, J. J. 1998, The Astronomical Journal, 115, 1693
Das, S., Kang, H., Ryu, D., & Cho, J. 2008, ApJ, 682, 29
Fang, K., & Olinto, A. V. 2016, ArXiv e-prints
Fukushima, M. 2015, EPJ Web Conf., 99, 04004
Gonzalez, A. H., Sivanandam, S., Zabludoff, A. I., & Zaritsky, D. 2013, Astrophys.J., 778, 14
Greisen, K. 1966, Phys. Rev. Lett., 16, 748
Haverkorn, M. 2015, in Astrophysics and Space Science Library, Vol. 407, Magnetic Fields in Diffuse Media, ed. A. Lazarian, E. M. de Gouveia Dal Pino, & C. Melioli, 483
Hillas, A. M. 1984, Annual review of astronomy and astrophysics, 22, 425
Hopkins, P. F., Richards, G. T., & Hernquist, L. 2007, ApJ, 654, 731
Huchra, J. P., Macri, L. M., Masters, K. L., Jarrett, T. H., Berlind, P., Calkins, M., Crook, A. C., Cutri, R., Erdoğdu, P., Falco, E., George, T., Hutcheson, C. M., Lahav, O., Mader, J., Mink, J. D., Martimbeau, N., Schneider, S., Skrutskie, M., Tokarz, S., & Westover, M. 2012, The Astrophysical Journal Supplement, 199, 26
Kachelrieß, M., Serpico, P. D., & Teshima, M. 2007, Astroparticle Physics, 26, 378
Kalli, S., Lemoine, M., & Kotera, K. 2011, A&A, 528, A109+
Kotera, K., & Lemoine, M. 2008, Phys. Rev. D, 77, 123003
Kotera, K., & Olinto, A. V. 2011, Ann. Rev. Astron. Astrophys., 49, 119
Lemoine, M., & Waxman, E. 2009, JCAP, 11, 009
Longair, M. S. 2011, High Energy Astrophysics
Mauch, T., Murphy, T., Buttery, H. J., Curran, J., Hunstead, R. W., Piestrzynski, B., Robertson, J. G., & Sadler, E. M. 2003, MNRAS, 342, 1117
McBride, J., Fakhouri, O., & Ma, C.-P. 2009, Mon.Not.Roy.Astron.Soc., 398, 1858
Merloni, A., & Heinz, S. 2007, MNRAS, 381, 589
Murase, K., Inoue, S., & Nagataki, S. 2008, Astrophys. J., 689, L105
Murase, K., & Takami, H. 2009, ApJ Letters, 690, L14
Nakamura, M., Tregillis, I. L., Li, H., & Li, S. 2008, ApJ, 686, 843
Oikonomou, F., Kotera, K., & Abdalla, F. B. 2015, JCAP, 1, 030
Planck Collaboration, Ade, P. A. R., Aghanim, N., Arnaud, M., Ashdown, M., Aumont, J., Baccigalupi, C., Banday, A. J., Barreiro, R. B., Bartlett, J. G., & et al. 2015, ArXiv e-prints
Rouillé d'Orfeuil, B., Allard, D., Lachaud, C., Parizot, E., Blaksley, C., & Nagataki, S. 2014, A&A, 567, A81
Ryu, D., Kang, H., & Biermann, P. L. 1998, A&A, 335, 19
Sambruna, R. M., Maraschi, L., & Urry, C. M. 1996, ApJ, 463, 444
Sheth, R. K., & Tormen, G. 1999, MNRAS, 308, 119
Takami, H., & Murase, K. 2012, ApJ, 748, 9
Ueda, Y., Akiyama, M., Hasinger, G., Miyaji, T., & Watson, M. G. 2014, ApJ, 786, 104
Urry, C. M., & Padovani, P. 1995, Publications of the Astronomical Society of the Pacific, 107, 803
van Velzen, S., Falcke, H., Schellart, P., Nierstenhöfer, N., & Kampert, K.-H. 2012, A&A, 544, A18
Vasudevan, R. V., Mushotzky, R. F., Winter, L. M., & Fabian, A. C. 2009, MNRAS, 399, 1553
Waxman, E. 1995, Physical Review Letters, 75, 386
Waxman, E., & Loeb, A. 2009, JCAP, 8, 026
Waxman, E., & Miralda-Escudé, J. 1996, ApJl, 472, L89+
Zatsepin, G., & Kuzmin, V. 1966, J. Exp. Theor. Phys. Lett., 4, 78